Dynamic Modeling of Magnetic Hysteresis

J. M. WHISNANT,* D. K. ANAND,† V. L. PISACANE,‡ AND M. STURMANIS*
The Johns Hopkins University, Applied Physics Laboratory, Silver Spring, Md.

Magnetic hysteresis rods have been used successfully for damping the attitude motions of passively stabilized near-Earth satellites. This paper describes the implementation of a model of magnetic hysteresis that is suitable for digital computer simulations of such motions. The model is based on the domain theory of magnetization which assumes that associated with each domain is a shifted rectangular hysteresis loop. Coefficients used by the model are determined by least-squares fitting data from experimental hysteresis loops. For a type of hysteresis rod commonly in use, it is shown that a simplified version of the model may be used. Results from the theoretical model are compared with experimentally generated loops and show good agreement.

Nomenclature

a,b ≡ axes of increasing and decreasing H in the theoretical hysteresis model
B ≡ magnetic flux density in a damping rod
B_n ≡ $B(H_n)$, the normal flux density in a rod
B_r ≡ $B(H_r) = B(0)$, the residual flux density in a rod
dA = weighted differential area in the Preisach plane
F ≡ function minimized in determining k_0 and the k_{ij}'s
H ≡ ambient magnetic field component along the longitudinal axis of a damping rod
H_n ≡ normal magnetizing force along the axis of a rod
H_r ≡ 0, the residual magnetizing force along the axis of a rod
k_0,k_{ij} ≡ coefficients determined by least-squares fitting experimental data to the theoretical model
N ≡ parameter that determines the order of the polynomials P_{ij}
P_{ij} ≡ polynomials in terms of H and H_n used in the theoretical model
α_{ij},β_{ij} ≡ coefficients of H_n when only the normal and residual experimental magnetization data are used
φ ≡ weighting function in the theoretical model

Introduction

THE method of utilizing in a passive sense the Earth's gravitational and magnetic fields to establish a desired spacecraft orientation has been highly successful. In some cases[1,2] the damping system consisted of permeable rods of predetermined magnetic characteristics. As the rods experience a varying magnetic field, magnetization and demagnetization of the rods results in hysteretic losses.[3] The hysteresis phenomenon is particularly well suited for satellite applications since the energy loss per cycle depends on the amplitude of oscillations rather than the rate. For gravity-gradient and geomagnetically stabilized satellites, the librational frequencies are comparable in magnitude to the orbital frequency. Permeable rods also have been used successfully in removing initial satellite spin before gravity or magnetic capture.[1] The spin rate of a satellite with hysteretic damping decreases linearly with time until it reaches zero. Thus rapid decay of low spin rates may be achieved.

Received August 13, 1969; revision received February 16, 1970. This work was done under Navy Contract NOw 62-0604-c. The authors would like to thank P. P. Pardoe who also was involved in the initial analytical work.

* Associate Mathematician, Space Research and Analysis Branch.

† Senior Staff, Space Research and Analysis Branch; also Associate Professor of Mechanical Engineering, University of Maryland. Member AIAA.

‡ Supervisor, Theory Project, Space Research and Analysis Branch. Member AIAA.

Hysteresis rod damping systems are low in cost and completely passive in that they require no sensing devices or electronics, use no power, and contain no moving parts. Passive damping offers the significant advantages of high reliability and a long lifetime.

The equations for the attitude motions of Earth-orbiting satellites, including perturbing forces due to the space environment, are well covered in the literature.[4] Consequently they will not be presented here. Since in general these equations must be integrated numerically by means of a digital computer, a model of the damping system is required. Analytical models of magnetic hysteresis exist for special cases such as a sinusoidally varying magnetic field where only symmetric major loops are produced. However, in satellite applications the magnetic field variations produce both major and minor loops, most of which are not symmetric. The modeling of hysteresis damping for satellite applications by digital techniques has received considerable attention.[5–8] Accurate models usually are accompanied by a high cost in computing time. Although one technique overcomes most of the problems associated with modeling hysteresis, it requires an inline hybrid computer.[8] Here, the implementation of a model of magnetic hysteresis that is suitable for digital simulation of satellite attitude motions is presented. In order to determine the effectiveness of the model, the theoretical results are compared with experimental data.

Modeling of Magnetic Hysteresis

An accurate analytical representation of magnetic hysteresis is extremely difficult, if not impossible, thereby necessitating the use of numerical methods. Any reasonable representation requires a model that includes the ability to preserve the history of the effect of variations in the magnetic field.[9] The theoretical model described here is attributed to F. Preisach[10,11] and is based on the domain theory of magnetization. It is assumed that the hysteretic material consists of infinitesimal volume elements, each characterized by a shifted rectangular hysteresis loop with coercive force $(a - b)/2$ and shift $(a + b)/2$ where a and b are as shown in Fig. 1. The volume elements, or domains, can be separated into two classes[11]: 1) domains for which a and b both have the same algebraic sign. These domains have a known direction of magnetization when $H = 0$; 2) domains for which a and b have different signs. The direction of magnetization for these domains when $H = 0$ is history dependent. In general, two different volume elements will have different values of a and b. The set of all values (a, b) corresponding to some hysteretic material comprises a region in the ab plane where only $a > b$ need be considered. Thus the model utilizes the triangular-shaped area which is illustrated in Fig. 2 and

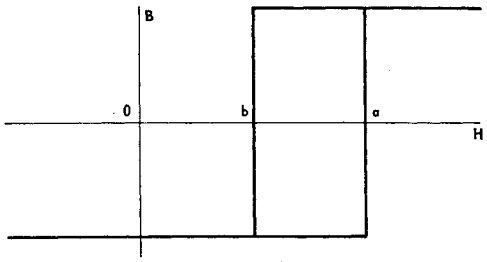

Fig. 1 Elemental rectangular hysteresis loop.

known as the Preisach plane. If the hysteretic material is demagnitized by an a.c. decreasing field, the volume elements go to positive magnetization for $a < -b$ and to negative magnetization for $a > -b$. This is also shown in Fig. 2.

Starting from the demagnetized condition, if H increases from $H = 0$ to $H = H_n$ then all negatively magnetized elemental rectangular loops for which $0 \leq a \leq H_n$ will flip to positive magnetization. The change in the magnetization of the material is thus related to the number of domains whose values of a and b lie in area A_1 of Fig. 3. If, instead, H decreases from $H = 0$ to $H = -H_n$ then all positively magnetized loops for which $-H_n \leq b \leq 0$ will flip to negative magnetization. This time the change in magnetization is related to the number of domains whose values of a and b lie in area A_2 of Fig. 3. Thus for a change in H, there is a relationship between the corresponding change in magnetization B and an area in the Preisach plane. A suitable definition of this relationship will yield a theoretical model of magnetic hysteresis. It is noted that the axes a and b are the axes of increasing and decreasing H, respectively.

Suppose that for each a and b in the triangular array there is a weighting function $\varphi(a,b)$ that is related to the statistical weight, or frequency, of rectangular loops characterized by a and b. The expression for the area differential in the Preisach plane will then be given by

$$dA = \varphi(a,b)dadb \tag{1}$$

The following, taken from Ref. 9, defines the relationship between changes in B and the weighted areas in the Preisach plane for the theoretical model under consideration here. If the ambient field component along the axis of a hysteresis rod is increased monotonically from zero to $+H_n$, then decreased monotonically to $-H_n$, and then increased to $+H_n$ again, the hysteresis loop illustrated in Fig. 4 is obtained. Points 1 and 3 are on the normal magnetization curve and have normal magnetizations B_n^+ and B_n^-. The B_n are obtained from the weighted areas illustrated in Fig. 3 and calculated from

$$B_n^+ = B(+H_n) = k_0H_n + \int_0^{H_n}\int_{-a}^{a} dA \tag{2}$$

and

$$B_n^- = B(-H_n) = k_0(-H_n) - \int_{-H_n}^{0}\int_{b}^{-b} dA \tag{3}$$

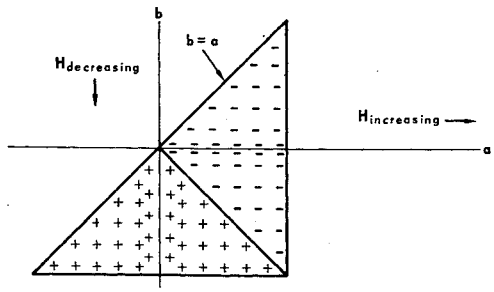

Fig. 2 Theoretical array (Preisach plane).

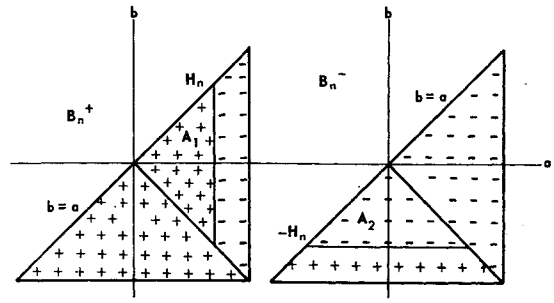

Fig. 3 Normal magnetization.

where $dA = \varphi(a,b)\ dadb$ and k_0 is the permeability of the hysteretic material in the vicinity of the origin. Note that the sign of the area for negative normal magnetization was set negative in Eq. (3). Points 2 and 4, which correspond to $H = 0$, are on the residual magnetization curve and have residual magnetizations B_r^+ and B_r^-. The B_r are obtained from the weighted areas illustrated in Fig. 5 and calculated from

$$B_r^+ = B(0,H_n) = \int_0^{H_n}\int_{-a}^{0} dA \tag{4}$$

and

$$B_r^- = B(0,-H_n) = -\int_{-H_n}^{0}\int_{0}^{-b} dA \tag{5}$$

Similarly, the expression for any B between $B(H_n)$ and $B(-H_n)$ is

$$B(H,H_n) = k_0H + \int_0^{H_n}\int_{-a}^{a} \varphi dbda - \int_H^{H_n}\int_b^{H_n} \varphi dadb \tag{6}$$

For the general case where H is increased from zero to H_1, decreased to H_2, and then increased to H_3, the corresponding magnetic induction $B(H_3)$ is obtained from

$$B(H_3) = k_0H_3 + \int_1 dA - \int_2 dA + \int_3 dA \tag{7}$$

The sign of each integral in Eq. (7) was determined by the area boundary line $b = -a$ as illustrated in Fig. 6. Thus the history of the effect of variations in the applied magnetic field is being preserved.

From symmetry considerations, the weighting function φ is defined as

$$\varphi(a,b) = \sum_{i+j=0}^{N} k_{ij}(a-b)^i(a+b)^j \tag{8}$$

where N is a function of the desired accuracy and the k_{ij}'s are determined from experimental hysteresis loops. Since the complexity of the computations is proportional to N, for the model discussed here i and j are restricted to the range $0 \leq i + j \leq 4$. An extension of Preisach's work that also is concerned with the selection of φ is given in Ref. 12. Sub-

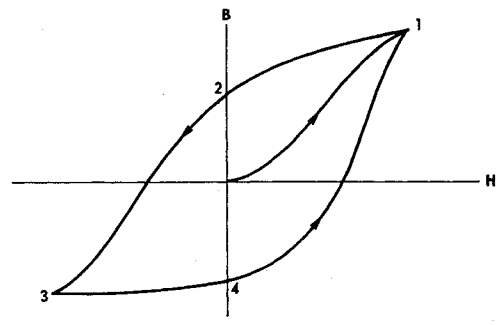

Fig. 4 Sample hysteresis loop.

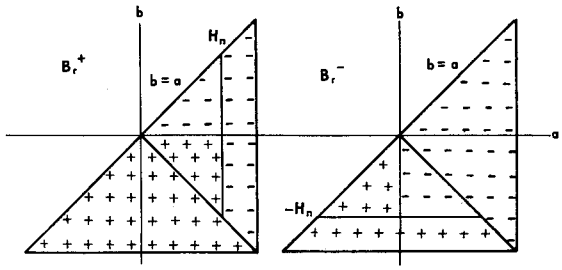

Fig. 5 Residual magnetization.

stitution of Eq. (8) into Eq. (6) yields

$$B(H,H_n) = k_0H + \sum_{i+j=0}^{N} k_{ij}P_{ij}(H,H_n) \qquad (9)$$

where the $P_{ij}(H,H_n)$ are polynomials of order $i + j + 2$. The polynomials through P_{20} are listed in the Appendix. The coefficients k_0 and the k_{ij}'s are obtained from a least-squares fit of Eq. (9) to the experimental magnetization data. This data is obtained by generating hysteresis loops, before the rods are placed in the spacecraft, for as many values of H_n as desired. The determination of k_0 and the k_{ij}'s for two specific cases is given next. The details of one procedure for performing the weighted area calculations on a digital computer are given in Ref. 9.

It is noted that for φ = constant ($N = 0$), the model described here reduces to that of Rayleigh.[13] For small values of H, he represented the sides of hysteresis loops by quadratic curves. The same result is obtained by substituting P_{00} from the Appendix into Eq. (9) and letting $N = 0$.

Specific Example and Results

Experience has shown that for the type of rods used in the APL satellites, use of the normal the residual magnetization data only is sufficient to accurately determine the k_{ij}'s. The rods are approximately 0.1 in. in diameter and consist of AEM 4750, a nickel-iron alloy. The rods studied varied in length from 30 to 54 in. For this case, the positive normal and residual values of B have the following form

$$B(H_n,H_n) = B_n^+ = k_0H_n + \sum_{i+j=0}^{N} k_{ij}(\alpha_{ij}H_n^{i+j+2}) \qquad (10)$$

$$B(H_r,H_n) = B_r^+ = \sum_{i+j=0}^{N} k_{ij}(\beta_{ij}H_n^{i+j+2}) \qquad (11)$$

For negative values of B, B_n^- and B_r^- are defined similarly. Thus the polynomials P_{ij} listed in the Appendix have reduced to the form $\alpha_{ij}H_n^{i+j+2}$ and $\beta_{ij}H_n^{i+j+2}$. The coefficients α_{ij} and β_{ij} for polynomials through sixth order in H_n are listed in Table 1. The discrepancies between Table 1 and the results of Ref. 9 are due to typographical errors in the latter.

Table 1 Coefficients of H_n^{i+j+2} in the determination of B_n^+ and B_r^+

		α_{ij}			
	$j = 0$	1	2	3	4
$i = 0$	1	2/3	2/3	4/5	16/15
1	2/3	1/3	4/15	4/15	
2	2/3	4/15	8/45		
3	4/5	4/15			
4	16/15				
		β_{ij}			
	$j = 0$	1	2	3	4
$i = 0$	1/2	1/6	1/12	1/20	1/30
1	1/2	1/6	1/12	1/20	
2	7/12	11/60	4/45		
3	3/4	13/60			
4	31/30				

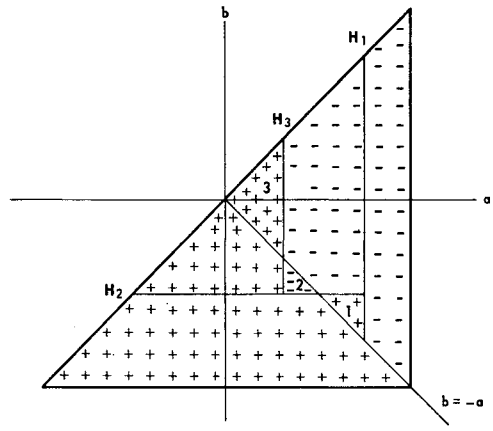

Fig. 6 Theoretical model and net areas used for $B(H_3) = k_0H_3 + \int_1 dA - \int_2 dA + \int_3 dA$.

Equations (10) and (11) determine the function to be minimized

$$F = \sum_{\substack{\text{all normal and} \\ \text{residual data}}} (B_n - B_{ne})^2 + (B_r - B_{re})^2 \qquad (12)$$

where the subscript e denotes experimental data. The minimization of F, in the least squares sense, yields the desired k_{ij}'s. Consider the experimental hysteresis loops shown in Figs. 7 and 8. The normal and residual magnetization data are used to determine the k_{ij}'s as listed on each figure. Determination of the k_{ij}'s along with Eq. (8) is used to produce the theoretical hysteresis loops also shown in the figures.

In the general case, the restriction of using only the normal and residual experimental magnetization data is removed and many data points along each hysteresis loop may be used to determine the k_{ij}'s. The minimization of F was achieved after changing Eq. (9) to orthogonal polynomial form. Several computer experiments indicated that $N = 4$ (sixth-order polynomials) was the optimum choice. A sample result is shown in Fig. 9.

Evaluation of the Model

The agreement between the theoretical model and experimental loops is good for the type of hysteresis rods currently

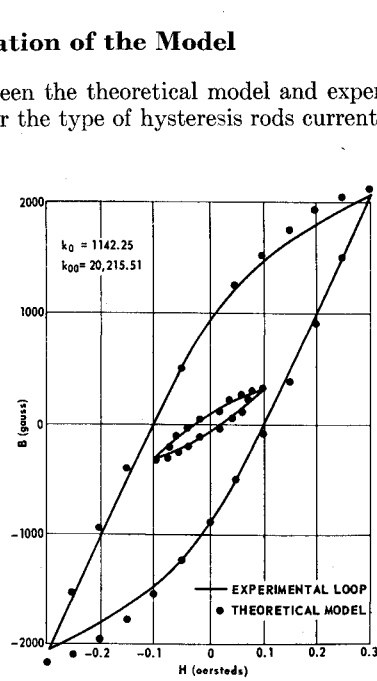

Fig. 7 Comparison between theoretical and experimental loops, 30-in. rod, $N = 0$.

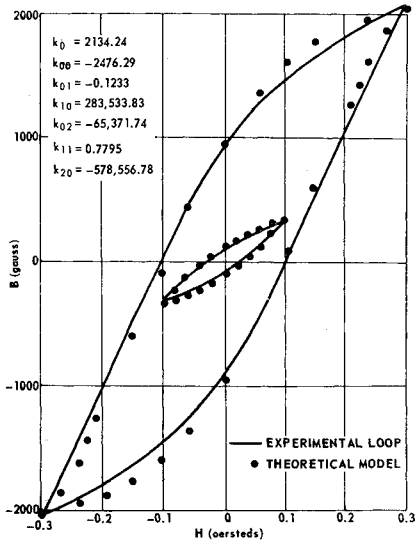

Fig. 8 Comparison between theoretical and experimental loops, 30-in. rod, $N = 2$.

being used in some of the APL satellites. For those rods, it is sufficient to use only the normal and residual magnetization data, as described previously, in determining the k_{ij}'s. Figs.

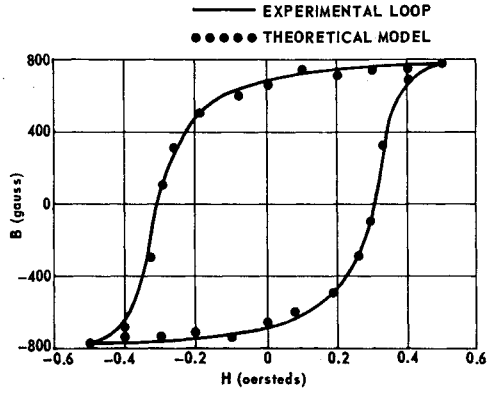

Fig. 9 Comparison between theoretical and experimental loops from an artificial hysteresis device, $N = 4$.

7 and 8 illustrate the comparison between experimental and theoretical hysteresis loops for a 30-in. rod for different size major loops and different values of N. A comparison between

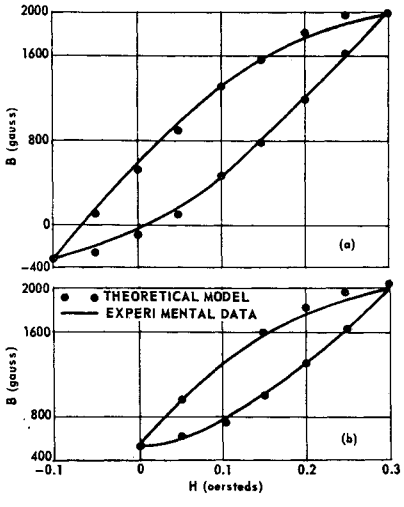

Fig. 10 Comparison between theoretical and experimental minor loops, $N = 1$.

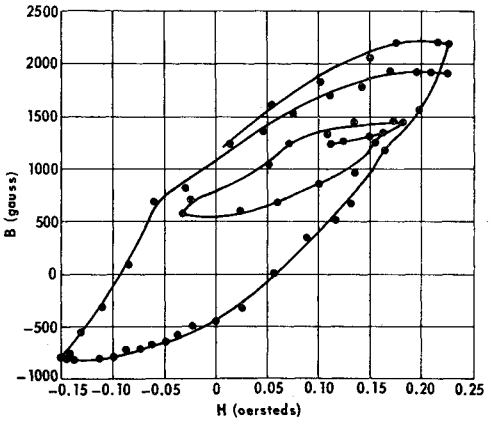

Fig. 11 Results from a simulation of a near-Earth satellite, 46-in. rod.

unsymmetrical minor loops for a different rod is shown in Fig. 10. The major limitation on the model is that the accuracy decreases for cases where the rods become saturated. However, it is usually desirable (and possible) to choose rods that do not become saturated anywhere in orbit. The model also may be used to simulate loops generated by artificial hysteresis devices.[14] A comparison between theoretical and experimental loops for such a device, using all the available magnetization data and $N = 4$, is shown in Fig. 9. Agreement with those types of hysteresis loops, usually more rectangular in shape, is not as good as that shown in Fig. 9 when only the normal and residual experimental magnetization data are used.

The hysteresis model described here has been programmed in subroutine form and is currently being used in the "Digital Attitude Simulation (DAS)" computer program.[9] DAS is a large-angle nonlinear simulation of the attitude motion of a spacecraft. Hysteresis loops generated by DAS during a simulation of a near-Earth (580 naut miles) satellite are shown in Fig. 11. B having been determined, the simulated torque due to the interaction of a hysteresis rod with the ambient magnetic field may then be computed and is proportional to $\bar{B} \times \bar{H}$. In orbit, the component of $\bar{H}$ along the axis of a rod frequently reverses itself, resulting in minor loops such as the one in Figure 11. Unfortunately, in-orbit experimental data corresponding to the theoretical results shown in Fig. 11 are not recorded. The only relevant in-orbit experimental datum available consists of a time history of the spacecraft's attitude motion. Hence, attitude results from DAS using the theoretical hysteresis model may be compared with the experimental attitude data. Previously,

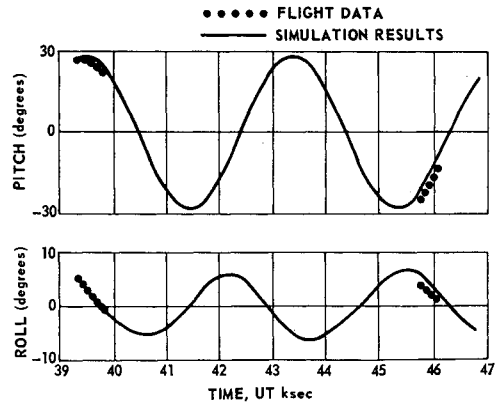

Fig. 12 Comparison of simulation and flight results for a near-Earth satellite with magnetic hysteresis damping, day 141, 1966.

DAS results have shown general agreement with attitude data from near-earth satellites with other forms of energy dissipation.[15] A comparison between simulation results and flight data for a near-Earth satellite with magnetic hysteresis damping is shown in Fig. 12. The agreement between the two results supports the validity of using this hystereisis model.

Costwise, attitude simulation runs for near-Earth satellites, including the effects of external perturbations, cost less than \$4 per orbit. The runs took 50% longer than the same simulations would have taken without hysteresis. The satellites considered have rods along each of two orthogonal axes. For satellites with rods along three axes or one axis, the simulation cost would change proportionately. Hence, while use of this hysteresis model is expensive, the cost is not prohibitive. Results of an investigation into cost-accuracy tradeoffs indicate that the cost of simulating hysteresis can probably be halved for only a slight loss in accuracy.

Appendix: Evaluation of the polynomials, $P_{ij}(H,H_n)$

For $0 \leq i + j \leq 2$, substituting Eq. (8) into Eq. (6) and performing the indicated integrations yields the following polynomials.

$$P_{00}(H,H_n) = (H_n^2/2) + H_nH - (H^2/2)$$

$$P_{01}(H,H_n) = (H_n^3/6) + (H_n^2H/2) + (H_nH^2/2) - (H^3/2)$$

$$P_{02}(H,H_n) = \frac{H_n^4}{12} + \frac{H_n^3H}{3} + \frac{H_n^2H^2}{2} + \frac{H_nH^3}{3} - \frac{7H^4}{12}$$

$$P_{10}(H,H_n) = (H_n^3/2) + (H_n^2H/2) - (H_nH^2/2) + (H^3/6)$$

$$P_{11}(H,H_n) = (H^4{}_n/6) + (H_n^3H/3) - (H_nH^3/3) + (H^4/6)$$

$$P_{20}(H,H_n) = \frac{7}{12}H_n^4 + \frac{H_n^3H}{3} - \frac{H_n^2H^2}{2} + \frac{H_nH^3}{3} - \frac{H^4}{12}$$

References

[1] Fischell, R. E., "Magnetic and Gravity Attitude Stabilization of Earth Satellites," CM-996, May 1961, Applied Physics Lab., Johns Hopkins Univ., Silver Spring, Md.

[2] Anand, D. K. et al., "Gravity-Gradient Capture and Stability in an Eccentric Orbit," *Journal of Spacecraft and Rockets*, Vol. 6, No. 12, Dec. 1969, pp. 1456–1459.

[3] Fischell, R. E., "Magnetic Damping of the Angular Motions of Earth Satellites," *ARS Journal*, Vol. 31, No. 9, Sept. 1961, pp. 1210–1217.

[4] Frick, R. H and Garber, T. B., "General Equations of Motion of a Satellite in a Gravitational Gradient Field," RM-2527, Dec. 1959, The Rand Corp., Santa Monica, Calif.

[5] *Magnetic Hysteresis Damping of Satellite Attitude Motions*, Doc. 64SD5242, Vols. 1 and 2, Nov. 1964, General Electric Co.

[6] Vanderslice, J. L., "Dynamic Analysis of Gravity-Gradient Satellite with Passive Damping," TG-502, June 1963, Applied Physics Lab., Johns Hopkins Univ., Silver Spring, Md.

[7] Chen, Y., "The Damped Angular Motion of a Magnetically Oriented Satellite," *Journal of the Franklin Institute*, Vol. 280, No. 4, Oct. 1965, pp. 291–306.

[8] Gluck, R. and Wong, A., "Inline Hybrid Computer for Simulation of Passively Stabilized Satellites," *Journal of Spacecraft and Rockets*, Vol. 6, No. 7, July 1969, pp. 812–818.

[9] Pardoe, P. P., "A Description of the Digital Attitude Simulation," TG-964, Feb. 1968, Applied Physics Lab., Johns Hopkins Univ., Silver Spring, Md.

[10] Becker, R. and Döring, W., *Ferromagnetismus*, Edwards Brothers, Ann Arbor, Mich. 1943, pp. 218–228.

[11] Preisach, F., "Uber die Magnetische Nachwirkung," *Zeitschrift fur Physik*, Vol. 94, 1935, pp. 277–302.

[12] Biorci, G. and Pescetti, D., "Analytical Theory of the Behavior of Ferromagnetic Materials," *Nuovo Cimento*, Vol. 7, No. 6, March 1958, pp. 829–842.

[13] Bozorth, R. M., *Ferromagnetism*, Van Nostrand, Princeton, 1951, pp. 489–494.

[14] Alper, J. R. and O'Neill, J. P., "A New Passive Hysteresis Damping Technique for Stabilizing Gravity-Oriented Satellites," *Journal of Spacecraft and Rockets*, Vol. 4, No. 12, Dec. 1967, pp. 1617–1622.

[15] Whisnant, J. M., Waszkiewicz, P. R., and Pisacane, V. L., "Attitude Performance of the GEOS-II Gravity-Gradient Spacecraft," *Journal of Spacecraft and Rockets*, Vol. 6, No. 12, Dec. 1969, pp. 1379–1384.